A Flexible Ultrasound Transducer with Tunable Focusing for Non-Invasive Brain Stimulation

Sunho Moon
The Department of Mechanical and Aerospace Engineering North Carolina State University
Raleigh, NC, USA
smoon4@ncsu.edu

Xiangming Xue
The joint Department of Biomedical Engineering North Carolina State University
Raleigh, NC, USA
xxue5@ncsu.edu

Mengyue Chen
The Department of Mechanical and Aerospace Engineering North Carolina State University
Raleigh, NC, USA
mchen23@ncsu.edu

Darpan Shukla
The Department of Mechanical and Aerospace Engineering North Carolina State University
Raleigh, NC, USA
dshukla2@ncsu.edu

Huaiyu Wu
The Department of Mechanical and Aerospace Engineering North Carolina State University
Raleigh, NC, USA
hwu15@ncsu.edu

Yong Zhu
The Department of Mechanical and Aerospace Engineering North Carolina State University
Raleigh, NC, USA
yzhu7@ncsu.edu

Wuwei Feng
The Department of Neurology Duke University School of Medicine
Durham, NC, USA
wayne.feng@duke.edu

Nitin Sharma
The joint Department of Biomedical Engineering North Carolina State University
Raleigh, NC, USA
nsharm23@ncsu.edu

Xiaoning Jiang
The Department of Mechanical and Aerospace Engineering North Carolina State University
Raleigh, NC, USA
xjiang5@ncsu.edu

2023 IEEE International Ultrasonics Symposium (IUS) | 979-8-3503-4645-9/23/$31.00 ©2023 IEEE | DOI: 10.1109/IUS51837.2023.10306786

***Abstract*—Transcranial focused ultrasound (tFUS) is promising for non-invasive brain stimulation, due to its millimeter-level spatial resolution and centimeter-level penetration depth. To stimulate various regions within the human brain, including cortical and subcortical structures, it is necessary to adjust the focal depth of a single-element focused ultrasound transducer. Common approaches involve the utilization of an acoustic lens, altering the curvature of transducer surface, or controlling the distance between the transducer and the scalp using either a water bag or a gel pad. However, such methods require multiple interchanges of lenses, transducers, or bags/pads, rendering them impractical for clinical applications. In this paper, we introduce a novel ultrasound stimulation device comprising a flexible ultrasound transducer and a precise movable plunger to enable focus tunability. The focused effect was simulated through finite element analysis, while the adjustability of focal depth was gauged by controlling interface curvature of the flexible transducer, as measured with hydrophone. This novel apparatus has the potential to enhance ease of use of tFUS and efficiency of its clinical applications.**

Keywords—Adjustable focus, Tunable focus, Flexible Ultrasound Transducers, Focused ultrasound, Transcranial focused ultrasound (tFUS)

I. INTRODUCTION

Transcranial ultrasound stimulation, employing transcranial focused ultrasound (tFUS), represents a non-invasive neuromodulation technology aimed at targeting both deep subcortical area and shallow cortical regions of intracranial brain [1]. tFUS is a promising technology for modulating human brain function and treating related dysfunctions owing to high spatial resolution and considerable penetration depth [1, 2]. However, a significant challenge arises when attempting to propagate ultrasound waves through a human skull for brain neuromodulation. This challenge is rooted in the acoustic mismatch between the skull and the scalp, resulting in ultrasound beam attenuation or distortion. This issue can be dealt with by using low-frequency ultrasound as frequencies surpassing 750 kHz can induce relatively diminished transmission efficiency of tFUS through the skull [3]. Moreover, in the context of neuromodulation applications, the single-element FUS transducer holds distinct advantages, including ease of use and cost-effectiveness [4]. Notably, the lateral resolution of the acoustic pressure field produced by a single element FUS transducer was even less than modular area of cortex [5].

Several techniques for acoustic focusing using single element ultrasound transducer involve acoustic liquid lens [6,7], Fresnel zone plate [8], and ultrasonic projector [9]. The physical manipulation of the acoustic field through the usage of a liquid lens and a Fresnel zone plate can facilitate the attainment of an adjustable focal length. Nevertheless, precision of transducer's performance when using a liquid lens is debatable. Due to the differences of acoustic impedance in materials between the liquid lens and water medium, leading to the measurement of delayed echoes with higher volumes of fluid within the liquid lens. The transducer featuring a Fresnel zone plate can function effectively in both air and water. Once the plate is fabricated, its focal length remains fixed. Even though the stretchable nature of the Fresnel zone plate allows for potential focus tunability, its stability of handling the plate can stands as a primary drawback [8]. The propagation direction of ultrasound waves can be easily controlled by altering the angle of acoustic projector, thereby facilitating the creation of a focused effect [9]. However, the unwieldy size and bulkiness hinders its clinical application.

Hence, we designed and fabricated a flexible ultrasound transducer comprising PZT-4/PDMS (polydimethylsiloxane) 1-3 piezoelectric composite. Following the findings in [3], a frequency of 650 kHz was selected, as it offers relatively improved tFUS transmission efficiency through the human skull and comparably narrower beamwidth. The focal adjustability of the transducer is facilitated by a suction gear comprised of a syringe (Inner Diameter: 40 mm), a plunger and a lead screw. This approach enables the curvature of the flexible transducer to be fine-tuned, achieving focus tunability. The flexible piezoelectric composite was characterized by measuring electrical impedance, pulse-echo response, and pulse-excitation response. Besides, a finite element analysis was conducted to appraise the acoustic output pressure at focal depth of 70 mm and at around 50 mm. Subsequently, the focused effect of acoustic beam profile was verified by utilizing the hydrophone. This concept culminates in a promising design for a focus-tunable ultrasound transducer, proficiently targeting diverse regions within cerebral cortex.

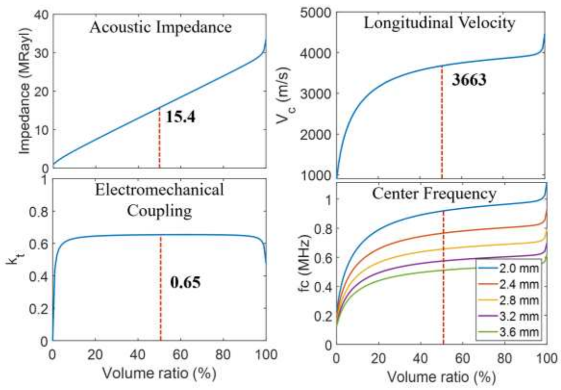

Fig. 1. Effective properties of PZT-4/PDMS 1–3 piezo-composite as a function of volume fractions.

II. Methods

A. Focus-Tunable Ultrasound Transducer Design

Similar to the previously reported work, a piezoelectric 1-3 composite was designed and fabricated with the dice-and-fill method. PZT-4 and PDMS were adopted as the active and filler material of the composite, respectively. The selection of PZT-4 as hard piezoelectric material stemmed from its mechanical durability and sufficiently high piezoelectric coefficient. The piezo-composite transducer with PDMS provides sufficient mechanical flexibility and biocompatibility. With theoretical design of material [10], the effective properties of PZT-4/PDMS piezoelectric 1-3 composite as function of volume fraction of PZT-4 were deduced, encompassing attributes such as acoustic impedance (Z), coupling coefficient (k), effective speed of sound, and thickness resonance frequency (f_r), all of which are depicted in Fig. 1. The adoption of a 50 % volume fraction was deemed, resulting in a pitch size of 1.7 mm and a kerf size of 0.5 mm. The transducer exhibited a center frequency of 650 kHz. the dimensions of 1-3 composite were chosen as 25 mm by 25 mm, based on krimholtz-leedom-matthae (KLM) simulations (BioSono, CA, US).

B. Focus-Tunable Ultrasound Transducer fabrication

Based on the simulated design parameters, PZT-4/PDMS 1-3 composite transducer was fabricated through the dice and fill technique. A PZT-4 disc (Steiner & Martins, Inc.) was first lapped to desired thickness of 2.8 mm by a lapping machine (Logitech Limited, UK) with accurate surface control on both sides. Subsequently, a Cr/Au (50/200 nm) electrode was deposited on the positive side. The 2.8 mm-thick PZT-4 was then diced into dimensions of 25 mm by 25 mm using 250-um thick dicing blade on the dicing machine (DAD 323, Disco, Japan). A representation of the cuts made on one side of the PZT-4 is shown in Fig. 2. (a). The resulting kerf gaps were meticulously cleansed with isopropyl alcohol. Liquid PDMS (Sylgard 184, Dow Corning) was formulated with a base-to-during agent weight ratio of 10:1. To eliminate the air bubbles generated during the mixing process, the PDMS was subjected to a 20-minute degassing treatment. During PDMS degassing, the conductive silver epoxy (E-Solder 3022, Von-Roll Inc.) was applied to the pillars to enhance adhesion with as-fabricated flexible silver nanowires (AgNW)/PDMS electrode (200 μm), fabricated using drop casting approach [12]. Subsequently, kerfs were filled with the degassed liquid PDMS up to the height of the PZT-4 pillars. The flexible AgNW/PDMS electrode was then affixed atop the 1-3 composite. Following overnight curing, the dice and fill method was repeated on the opposite side of 1-3 composite. After establishing the ground and positive wire connection, a 3D-printed holder was integrated with the flexible 1-3 composite (Fig. 2. (b)), culminating in its integration with the suction gear to enable focus tunability. Fig. 2. (c) shows the focus-tunable flexible ultrasound transducer.

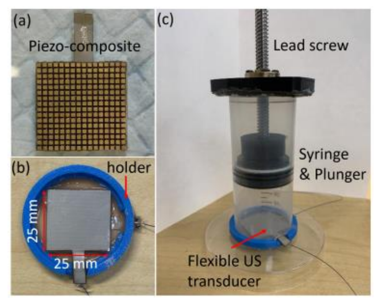

Fig. 2. PZT-4/PDMS 1-3 piezoelectric composite (a), flexible ultrasound transducer integrated with 3D printed holder (b), and focus tunable ultrasound transducer combined with suction gear (c)

C. Finite Element Analysis of Acoustic Output Pressure

Acoustic pressure fields produced by the 1-3 piezoelectric composite transducer were simulated using the commercial finite element software (COMSOL Multiphysics®). A voltage of 100 V (AC) and ground conditions were applied to the top and bottom surfaces of the piezoelectric pillars, respectively. Water was set as the acoustic media. The energy produced by mechanical vibration of the composite was transferred to the acoustic media through the fluid-structure interaction condition at the positive surfaces of the transducer. The pressure and the acoustic intensity output were computed at resonant frequency in a region of 100 mm for both flat mode and curved mode. Furthermore, the resolution of beam profile at focal length were estimated in conditions of flat mode and curved mode of focus-tunable transducer.

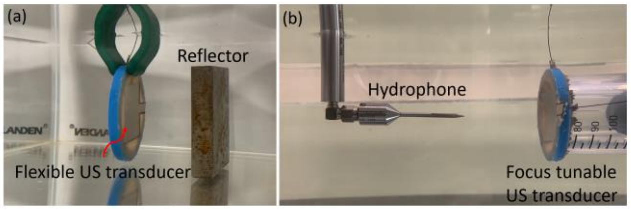

Fig. 3. Experimental setup for pulse-echo response (a) and pulse-exitation response (b).

D. Focus-Tunable Ultrasound Transducer characterization

The electrical impedance and phase angle as function of frequency were measured with an impedance analyzer (4294A, Agilent Tech. Inc., Santa Clara, CA). The capacitance and dielectric loss were derived using the same impedance analyzer. These parameters were compared between the transducer's flat mode and its curved mode (with a curvature radius of 46 mm). To further assess the performance of the focus tunable US transducer, both pulse-echo response and pulse-excitation response of the focus-tunable US transducer were simulated through a KLM model. The simulated results were compared with the corresponding experimental measurements.

The experiment set up for the Pulse/echo test is illustrated in Fig. 3. (a). A pulser and receiver (5077 PR, Olympus, WA, USA) was connected to the transducer, operating with a pulse repetition frequency (PRF) of 200 Hz and input voltage of 100 V. A steel bar was used as a reflector. An oscilloscope (DSO7104B, Agilent Technologies, Santa Clara, CA, USA) was used to display the radiofrequency (RF) signal. The experiment set up for pulse-excitation response is shown in Fig. 3. (b). A function generator (33250A, Agilent Tech. Inc., Santa Clara, CA) was connected to the power amplifier (75A250A, AR, Souderton, PA). The transducer was subjected to excitation, emitting 3 cycles of sinusoidal pulse with an input voltage of 100 V toward hydrophone (HGL-0085, ONDA Crop. Sunnyvale, CA) in a water tank. To assess spatial resolution at both the natural focus and curved focal length, hydrophone was installed on the 3D motor motion stage. The changes in peak-to-peak voltage were collected at 39 μs and 30 μs (corresponding focal point of 60 mm and 46 mm) along the x-axis, spanning from -12 mm to 12 mm in increments of 0.5 mm. Simultaneously, corresponding magnitudes of relative acoustic pressure were ascertained at focal lengths of 60 mm and 46 mm.

III. Results

A. Focus-Tunable Ultrasound Transducer characterization.

Fig. 4. (a – b) displays the measured electrical impedance of PZT-4/PDMS 1-3 composites across various frequencies. Considering the requirements for most US brain stimulation applications [3], a relatively large apertures and low frequency was applied for the transducer, which resulted in a relatively low electrical impedance of 20 Ω with the flat mode. Yet, this trade-off won't affect the flexibility study over the transducer and will be fixed with a tunning circuit after housing. In the curved mode with a radius of 46mm, the transducer showed an electrical impedance of 18 Ω corresponding to an 11 % deviation compared with the flat mode. There were no discernible distinctions in impedance spectra between the flat mode and the curved mode.

Fig. 4 (c – d) showed the simulated and measured results based on the fabricated flexible 1-3 composite. The measured results showed a P/E sensitivity of 50.4 mV/V with a center frequency around 605 kHz and -6 dB bandwidth of 18 %. The difference between the simulation and the fabrication may be due to the thickness control of the AgNW/PDMS electrode in front and rear of the transducer, which partly distorted the waveform. Yet, the deviations between simulation and measurement over frequency and sensitivity were less than 0.02 % and 0.06 %, respectively, which was not significant for the flexibility study.

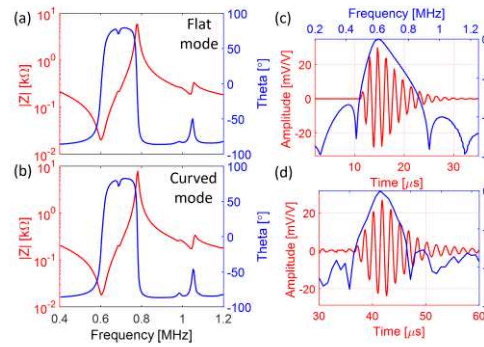

Fig. 4. the measured electrical impedance and phase angle of PZT-4/PDMS 1-3 composites across various frequencies in flat mode (a) and curved mode with curvature radius of 46 mm (b). Simulated (c) and measured (d) results for pulse-excitation response

B. Finite Element Analysis

Fig. 5 depicts the acoustic pressure fields at 650 kHz for the 1-3 composite transducer across different focal lengths. Examining the acoustic pressure fields for the flat mode, as shown in Fig. 5. (a), reveals a focal length at around 75 mm. In contrast, Fig. 5. (b) conveys the acoustic pressure fields for curved mode, featuring a 65 mm, 55 mm, and 45 mm curvature radius. Notably, the comparison between two modes indicates that the acoustic pressure within curved mode slightly exceeds that of the flat mode. This consequence can be attributed to the convergence of focused energy resulting from curvature.

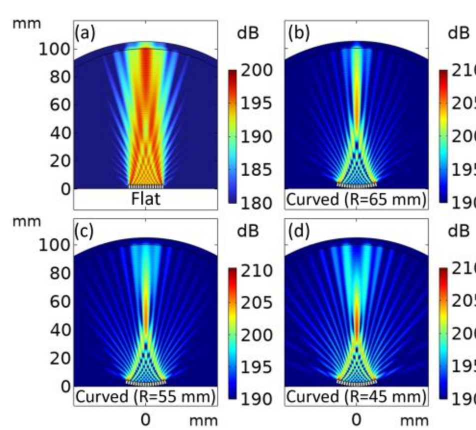

Fig. 5. the acoustic pressure fields for flat mode and curved mode

C. Hydrophone Test for Focused Effect Characterization

By controlling the syringe, the liquid volume at the back side of the transducer can be adjusted. The hydrophone recorded its maximum received voltage level at corresponding focal depth of 46 mm and 70 mm, which are the highest and lowest values of curvature employed in the simulation. Fig. 6 showcases the plotted relative magnitude of the acoustic pressure at focal lengths. Comparing the results for the flat and curved cases, the flat and curved mode showed -6 dB beamwidth of 15.5 mm and 12 mm. This indicated a 30% increase in lateral resolution for the curved case, allowing for more accurate control of the stimulation region. Additionally, in the curved mode, the acoustic pressure increased from 0.45 to 0.69 MPa, signifying a 35% enhancement in transmitting sensitivity compared to the flat mode.

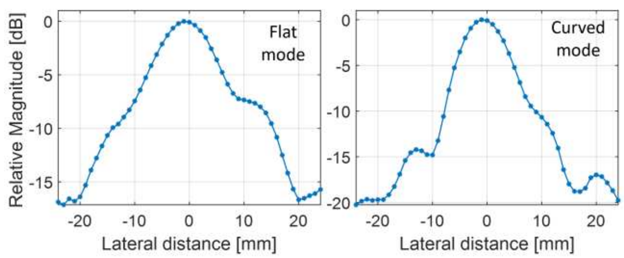

Fig. 6. Relative magnitude of the acoustic pressure at focal lengths of 70 mm (flat mode) and 46 mm (curved mode)

IV. Discussion

In this work, we developed the flexible ultrasound transducer with the ability to tune its focus. In terms of ultrasound acoustic pressure, simulation using finite element analysis indicated that maximum output pressure was achieved at around 75 mm focal length. However, experimental measurements using hydrophone revealed that the peak output pressure occurred at 60 mm focal length. This result aligns with the calculated natural focus depth for the transducer with an aperture size of 25 mm^2. This discrepancy could be attributed to the inherent characteristics of PDMS, causing a slight curvature in the flexible 1-3 composite transducer. Consequently, the actual focal length in flat mode was observed to be roughly 10 – 15 mm closer to the transducer compared to the focal length predicted by simulation results.

In a previous study [11], we examined the focused effect of transducer by bending it in the 1D curved condition. This assessment revealed a focused effect at a focal length of 6.5 mm. The focus tunable flexible ultrasound transducer, developed in this work, can be spherically curved, thereby achieving a focused effect with narrower beam width and higher pressure compared to the flat state of the transducer. Moreover, with the integration of suction gear, the flexible ultrasound transducer can achieve curvature up to 46 mm. Additional tests will be conducted to demonstrate the focus tunability of the flexible ultrasound transducer. This will involve mapping the acoustic pressure distribution in a curved condition with varying radii of curvature, offering further validation of the transducer's focal tunability.

V. Conclusion

This work introduced the flexible PZT-4/PDMS 1-3 piezoelectric composite was designed and fabricated as the transducer. Through integration with the suction gear consisting of syringe, plunger, and lead screw, the flexible transducer gained the remarkable ability of tunable focal depth. This focal length adjustment was achieved by controlling the lead screw's backward movement, allowing for reductions in focal length. The transducer was comprehensively characterized to evaluate electrical impedance, pulse-echo response, and pulse-excitation response. The acoustic beam profile at different focal depths was simulated via finite element analysis. By tunning the radius of transducer to 46 mm, improvement of 30 % and 35 % were achieved in resolution and transmitting sensitivity, respectively. These results indicate the potential of the flexible transducer for tunable brain neuromodulation applications.

Acknowledgment

This research is partially supported by grants from NCSU Research Innovation Seed Funding (RISF), NIH grant # R21EB032059, # 1R01HD108473, and NSF grant # 2124017.

References

[1] C. Hou et al., "An Optimized Miniaturized Ultrasound Transducer for Transcranial Neuromodulation," Frontiers in Neuroscience, vol. 16, Jun. 2022

[2] B. P. Mead et al., "Novel Focused Ultrasound Gene Therapy Approach Noninvasively Restores Dopaminergic Neuron Function in a Rat Parkinson's Disease Model," Nano Letters, vol. 17, no. 6, pp. 3533–3542, May 2017

[3] M. Chen et al., "Numerical and experimental evaluation of low‐intensity transcranial focused ultrasound wave propagation using human skulls for brain neuromodulation," Medical Physics, vol. 50, no. 1, pp. 38‐49, Nov. 2022

[4] Y. Tufail, A. Yoshihiro, S. Pati, M. M. Li, and W. J. Tyler, "Ultrasonic neuromodulation by brain stimulation with transcranial ultrasound," Nature Protocols, vol. 6, no. 9, pp. 1453–1470, Sep. 2011

[5] W. Legon et al., "Transcranial focused ultrasound modulates the activity of primary somatosensory cortex in humans," Nature Neuroscience, vol. 17, no. 2, pp. 322–329, Feb. 2014

[6] Z. Li et al., "Liquid lens with adjustable focus for ultrasonic imaging," Applied Acoustics, vol. 175, p. 107787, Apr. 2021

[7] F. Wang, Z. Zhuang, Z. Qin, and B. Wen, "Movable and Focus-Tunable Lens Based on Electrically Controllable Liquid: A Lattice Boltzmann Study," Entropy, vol. 24, no. 12, pp. 1714–1714, Nov. 2022

[8] X. Xia, Y. Li, F. Cai, H. Zhou, T. Ma, and H. Zheng, "Ultrasonic tunable focusing by a stretchable phase-reversal Fresnel zone plate," Applied Physics Letters, vol. 117, no. 2, p. 021904, Jul. 2020

[9] Z. Li et al., "Adjustable acoustic field controlled by 'ultrasonic projector' on ultrasound application," IEEE Transactions on Ultrasonics Ferroelectrics and Frequency Control, pp. 1–1, Jan. 2021

[10] W. H. Smith and B. A. Auld, "Modeling 1-3 composite piezoelectrics: thickness-mode oscillations.," IEEE Transactions on Ultrasonics Ferroelectrics and Frequency Control, vol. 38, no. 1, pp. 40–7, Jan. 1991

[11] T. Kim, Z. Cui, W.-Y. Chang, H. Kim, Y. Zhu, and X. Jiang, "Flexible 1–3 Composite Ultrasound Transducers With Silver-Nanowire-Based Stretchable Electrodes," IEEE Transactions on Industrial Electronics, vol. 67, no. 8, pp. 6955–6962, Aug. 2020

[12] F. Xu and Y. Zhu, "Highly Conductive and Stretchable Silver Nanowire Conductors," Advanced Materials, vol. 24, no. 37, pp. 5117–5122, Jul. 2012